Environmental Science & Technology

Article

pubs.acs.org/est

Hepatic Metabolism Affects the Atropselective Disposition of 2,2′,3,3′,6,6′-Hexachlorobiphenyl (PCB 136) in Mice

Xianai Wu,[†] Christopher Barnhart,[‡] Pamela J. Lein,[‡] and Hans-Joachim Lehmler*,[†]

[†]Department of Occupational and Environmental Health, College of Public Health, The University of Iowa, Iowa City, Iowa 52242, United States

[‡]Department of Molecular Biosciences, School of Veterinary Medicine, University of California, Davis, California 95616, United States

Supporting Information

ABSTRACT: To understand the role of hepatic vs extrahepatic metabolism in the disposition of chiral PCBs, we studied the disposition of 2,2′,3,3′,6,6′-hexachlorobiphenyl (PCB 136) and its hydroxylated metabolites (HO-PCBs) in mice with defective hepatic metabolism due to the liver-specific deletion of cytochrome P450 oxidoreductase (KO mice). Female KO and congenic wild type (WT) mice were treated with racemic PCB 136, and levels and chiral signatures of PCB 136 and HO-PCBs were determined in tissues and excreta 3 days after PCB administration. PCB 136 tissue levels were higher in KO compared to WT mice. Feces was a major route of PCB metabolite excretion, with 2,2′,3,3′,6,6′-hexachlorobiphenyl-5-ol being the major metabolite recovered from feces. (+)-PCB 136, the second eluting PCB 136 atropisomers, was enriched in all tissues and excreta. The second eluting atropisomers of the HO-PCBs metabolites were enriched in blood and liver; 2,2′,3,3′,6,6′-hexachlorobiphenyl-5-ol in blood was an exception and displayed an enrichment of the first eluting atropisomers. Fecal HO-PCB levels and chiral signatures changed with time and differed between KO and WT mice, with larger HO-PCB enantiomeric fractions in WT compared to KO mice. Our results demonstrate that hepatic and, possibly, extrahepatic cytochrome P450 (P450) enzymes play a role in the disposition of PCBs.

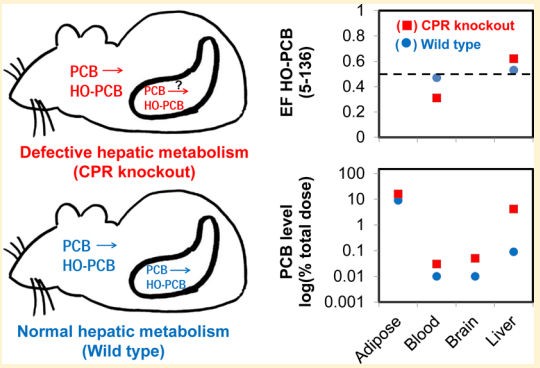

INTRODUCTION

Although the industrial production of polychlorinated biphenyls (PCBs) has been banned worldwide under the Stockholm Convention,[1] PCBs still represent a significant environmental and human health concern. Specifically, PCBs continue to be released into the environment from building materials and other sites of PCB use.[2] Electronic waste processing has resulted in considerable environmental and occupational PCB exposure at electronic waste sites around the world.[3−5] Several recent studies revealed the presence of PCBs in certain paint pigments,[6,7] highlighting the fact that the inadvertent production of PCBs by industrial processes represents a current, environmental source of PCBs. There is increasing evidence that, in particular, PCB congeners with multiple *ortho* chlorine substituents predominate in outdoor[2] and indoor air,[2,8] environmental[9,10] and human samples.[11−13] These *ortho*-substituted PCB congeners and their hydroxylated metabolites are endocrine disruptors[14] and have been implicated as developmental neurotoxicants by mechanisms involving altered Ca^{2+} signaling, interference with thyroid hormone signaling, and decreased dopamine content.[15−17]

In vitro metabolism studies have shown that PCBs are oxidized by P450 enzymes to HO-PCBs. The P450 isoforms involved in the metabolism of a particular PCB congener depend on its chlorine substitution pattern. PCB congeners with *ortho* substituents are typically metabolized by phenobarbital-inducible CYP2B enzymes,[18−22] whereas PCB congeners without *ortho* substituents are metabolized by CYP1A enzymes.[23] Several environmentally relevant PCB congeners (e.g., PCB 136) are chiral because they exist as rotational isomers, or atropisomers, that are nonsuperimposable mirror images of each other. Atropselective metabolism of these chiral PCB congeners by P450 enzymes is thought to result in their atropisomeric enrichment in wildlife, laboratory animals, and humans.[24] HO-PCBs may be further metabolized in the liver to dihydroxylated metabolites or glucuronide and sulfate conjugates.[18,25−27] There is experimental evidence from *in vitro* studies using recombinant P450 enzymes that the oxidation of HO-PCBs to dihydroxylated metabolites is also atropselective.[18] It is likely that glucuronide or sulfate conjugates of HO-PCBs are also formed atropselectively; however, this has not been shown experimentally.

Received: September 29, 2014
Revised: November 21, 2014
Accepted: November 24, 2014
Published: November 24, 2014

   dx.doi.org/10.1021/es504766p | Environ. Sci. Technol. 2015, 49, 616−625

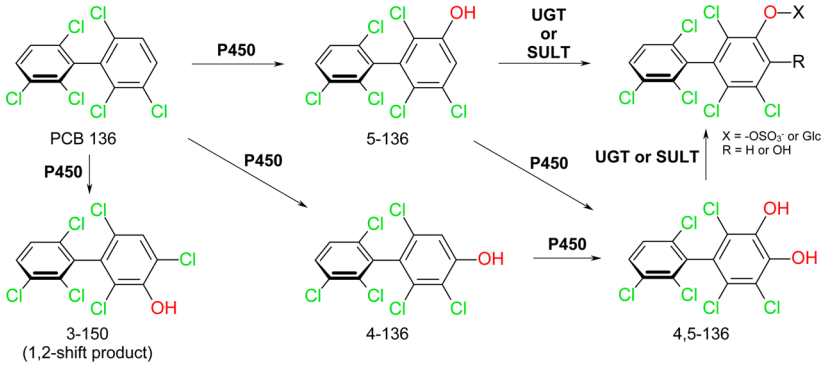

Figure 1. Simplified metabolism scheme of PCB 136 atropisomers showing major HO-PCB metabolites investigated and the corresponding abbreviations. Only one atropisomer of PCB 136 and the corresponding metabolites are shown for clarity reasons. P450, cytochrome P450 enzyme; UGT, uridine 5′-diphospho-glucuronosyltransferase; SULT, sulfotransferase; Glc, glucuronide.

Despite a large number of *in vitro* metabolism studies,[18−23] the importance of hepatic vs extrahepatic P450 enzymes for the atropselective metabolism and excretion of PCB 136 and its HO-PCB metabolites remains unproven *in vivo*. To address this knowledge gap, the present study uses a genetic mouse model with defective hepatic metabolism due to the liver-specific deletion of the cytochrome P450 reductase (*cpr*) gene to investigate the role of hepatic metabolism in the atropselective disposition of PCB 136 and its metabolites in mice. In this mouse model all P450 isoforms involved in the hepatic metabolism of PCBs are inactivated or inhibited because CPR, the required electron donor of all microsomal P450 enzymes, is not expressed in the liver. PCB 136 was selected for this disposition study because it is a chiral PCB congener of environmental relevance[24] and atropspecifically alters neuronal connectivity in rat hippocampal neurons by mechanisms involving ryanodine receptors.[28]

EXPERIMENTAL PROCEDURES

Chemicals. Analytical standards of 2,3,4′,5,6-pentachlorobiphenyl (PCB 117), 2,2′,3,4,4′,5,6,6′-octachlorobiphenyl (PCB 204), and 2,3,3′,4,5,5′-hexachlorobiphenyl-4′-ol (4′-159) were purchased from AccuStandard (New Haven, CT, USA). 2,2′,3,3′,6,6′-Hexachlorobiphenyl (PCB 136) and the corresponding HO-PCB metabolites (2,2′,3′,4,6,6′-hexachlorobiphenyl-3-ol, 3-150; 2,2′,3,3′,6,6′-hexachlorobiphenyl-4,5-diol, 4,5-136; 2,2′,3,3′,6,6′-hexachlorobiphenyl-4-ol, 4-136; 2,2′,3,3′,6,6′-hexachlorobiphenyl-5-ol, 5-136) were synthesized as described earlier.[21,29] The respective structures and abbreviations are shown in Figure 1. Diazomethane for the derivatization of HO-PCBs to methoxylated PCBs was synthesized from *N*-methyl-*N*-nitroso-*p*-toluenesulfonamide (Diazald) using an Aldrich mini Diazald apparatus (Milwaukee, WI, USA).[30]

Mouse Model Maintenance and Characterization. Alb-Cre$^{\pm}$/Cpr$^{lox+/+}$ mice with liver-specific deletion of the cytochrome P450 oxidoreductase (EC 1.6.2.4) gene (KO) and congenic Alb-Cre$^{-/-}$/Cpr$^{lox+/+}$ mice (wild type, WT) were obtained from Dr. Xinxin Ding (School of Public Health, State University of New York, Albany, NY) to establish a breeding colony at the University of Iowa.[31,32] Breeding pairs were set up between KO and WT mice, and littermates were genotyped by PCR in the University of Iowa Transgenic Animal Facility as described previously.[31] Animals were housed in standard plastic cages in a controlled environment maintained at 22 °C with a 12 h light−dark cycle. The mice were fed a basal diet (Harlan 7913 with 18% protein, 6% fat, and 5% fiber) and water ad libitum. Housing of breeding pairs and animal experiments were approved by the Institutional Animal Care and Use Committee at the University of Iowa (protocol #1206120).

Liver microsomes were prepared from eight week old, naïve (i.e., untreated) female KO (n = 6) and WT mice (n = 5) using established procedures[20] to characterize the effects of the liver-specific deletion of *cpr* on total P450 levels and hepatic CPR, CYP1A, and CYP2B activities (for additional experimental details, see Table S1). The effects of the liver-specific deletion on these markers were consistent with published findings.[31] In particular, a drastically reduced CPR activity was observed in the liver of KO compared to WT mice. In contrast, liver-specific deletion of *cpr* did not significantly alter the expression of synaptic plasticity-associated genes (i.e., activity-regulated cytoskeleton-associated protein, myelin basic protein, neurogranin, and spinophilin) in the cortex, hippocampus, or cerebellum of KO compared to WT mice (Table S2).

PCB 136 Disposition Study. KO and congenic WT mice (8 week old females) were obtained from the breeding colony described above and randomly divided into the following treatment and control groups (Table S3): 1) WT mice (n = 4) received a single oral dose of PCB 136 (30 mg/kg b.w.) on a Vanilla Wafer cookie (7.5 g/kg b.w.); 2) KO mice (n = 7) received a single oral dose of PCB 136 (30 mg/kg b.w.) on a Vanilla Wafer cookie (7.5 g/kg b.w.); 3) WT control mice (n = 5) received the vehicle (cookie; 7.5 g/kg b.w.) alone; and 4) KO control mice (n = 5) received the vehicle (cookie; 7.5 g/kg b.w.) alone. The dosing of all mice using a cookie was performed as described previously.[33] After eating the entire cookie, animals were housed individually in metabolic cages, and urine and feces were collected daily from each animal for 3 days. After 3 days, mice were euthanized by CO_2 asphyxiation followed by cervical dislocation. Blood was collected by cardiac puncture into glass vials. Tissues (brain, liver, and adipose tissue) were excised *en bloc*, and their wet weight was determined. PCB treatment had no significant effect on body or organ weights (Table S3). All samples were stored at −80 °C until further analysis.

Extractable Lipid Content in Tissues. Lipids were extracted from tissues (liver, brain, and adipose tissue) and feces of PCB or vehicle-treated animals by pressurized liquid extraction using a Dionex ASE200 system (Dionex, Sunnyvale, CA) as described earlier.[33] Briefly, the samples were mixed with 2 g of diatomaceous earth (Fisher Scientific) and placed in ASE extraction cells (11 mL). The cells were extracted using a

dx.doi.org/10.1021/es504766p | Environ. Sci. Technol. 2015, 49, 616−625

chloroform/methanol mixture (2:1, *v/v*) at 120 °C and 1500 psi. The lipid content was determined gravimetrically after evaporation of the solvent. The extractable lipid content of each tissue or feces are summarized in Table S4.

PCB 136 and Metabolite Extraction Procedures. PCB 136 and its hydroxylated metabolites were extracted by pressurized liquid extraction from liver (0.30−0.74 g), brain (0.19−0.30 g), adipose (0.04−0.29 g), and feces samples (0.61−0.75 g) from individual mice using a Dionex ASE200 system following a published method with modifications.[29] Briefly, the tissues were mixed with diatomaceous earth (2 g) and placed in the extraction cell (33 mL) containing Florisil (60−100 mesh, 12 g; Fisher Scientific). PCB 117 (250 ng) and 4′-159 (137 ng) were added to each sample as surrogate standards, and the cells were extracted with hexane-dichloromethane-methanol (48:43:9, v/v/v) at 100 °C and 1500 psi (10 MPa) with preheat equilibration for 6 min, 60% of cell flush volume, and 1 static cycle of 5 min. Sample blanks containing only Florisil and diatomaceous earth were extracted in parallel with each sample set. The extracts were concentrated to approximately 1 mL using a Turbo Vap II (Biotage, LLC, NC, USA) and transferred with 1 mL of hexane to glass tubes. The solvent was evaporated to dryness under a gentle stream of nitrogen and redissolved in 1 mL of hexane. After derivatization of the HO-PCBs with diazomethane, the organic extracts were subjected to a sulfur cleanup step as described earlier, followed by treatment with concentrated sulfuric acid and addition of the internal standard (PCB 204).[33]

PCB 136 and its hydroxylated metabolites were extracted from blood samples (0.49−0.87 g) from individual mice by liquid−liquid extraction as described previously.[34] Briefly, blood samples were diluted with aqueous KCl (1%; 3 mL). The surrogate standards (PCB 117 and 4′-159, 50 ng each) were added to each sample. Samples were acidified with HCl (6 M; 1 mL), followed by addition of 2-propanol (3 mL). Samples were extracted with hexane: MTBE (1:1, *v/v*; 5 mL) and hexane (3 mL). The combined organic extracts were washed with aqueous KCl (1%; 3 mL), evaporated to dryness, derivatized with diazomethane, and further treated as described above for tissue and feces samples.

PCB 136 and Metabolite Extraction from Urine Samples. Two aliquots of each urine sample (0.2 mL) were diluted with an equal volume of 0.2 M sodium acetate buffer (pH = 5). To determine if glucuronide and/or sulfate conjugates of PCB 136 were present in urine samples both aliquots were incubated in parallel with or without *β*-glucuronidase/sulfatase mixture (20 *μ*L; type H-2 from *Helix pomatia*, 100,000 units/mL; Sigma-Aldrich Co. St. Louis, MO, USA) for 12 h at 37 °C.[35] Subsequently, PCB 136 and its hydroxylated metabolites were extracted from urine samples as described above for blood.

Gas Chromatographic Analysis of PCB 136 and Its Metabolites. Analysis of PCB 136 and the methylated derivatives of hydroxylated PCB 136 metabolites was performed on a DB1-MS (60 m × 0.25 mm ID × 0.25 *μ*m film thickness; Agilent, Santa Clara, CA) or an Equity-1 capillary column (60 m × 0.25 mm ID × 0.25 *μ*m film thickness; Supelco, Bellefonte, PA) using an Agilent 7890A gas chromatograph equipped with two ^{63}Ni-*μ*ECDs as described previously.[36] The levels of PCBs were calculated using PCB 204 as internal standard, adjusted for surrogate recoveries, and are presented adjusted for tissue wet weight, lipid content, and as percent of the total PCB 136 dose (Tables S7−S11).

Enantiomeric fractions, a measure of the atropisomeric enrichment of PCB 136 and its metabolites, were determined on the same instrument described above. If not stated otherwise (see Table S12), enantioselective determinations were performed with extracts from tissues or excreta collected from individual animals. Briefly, PCB 136 and 5-136 atropisomers were separated using a ChiralDex BDM column (BDM column, 30 m × 250 *μ*m × 0.12 *μ*m; Supelco, Analytical, St. Louis, MO).[20] The temperature program was as follows: 10 °C/min from 100 to 148 °C, hold for 400 min, 10 °C/min to 200 °C, and hold for 13 min. PCB 136 and 4-136 atropisomers were separated with a Cyclosil-B column (CB column, 30 m × 0.25 mm ID × 0.25 *μ*m film thickness; Agilent, Santa Clara, CA, US) using a previously published temperature program.[20] Atropisomers of 4,5-136 did not resolve on either atropselective column. To allow a comparison with previously published data,[33,37−40] the EF values were determined as EF = Area E_2/(Area E_1 + Area E_2), were Area E_1 and Area E_2 denote the peak area of the first and second eluting atropisomer. On both enantioselective columns, E_1-PCB 136 and E_2-PCB 136 correspond to (−)-PCB 136 and (+)-PCB 136, respectively.[41,42] The E_1- and E_2-atropisomers of 5-136 (BDM column) and 4-136 (CB column) are formed from (−)- and (+)-PCB 136, respectively.[20] The EF values of PCB 136, 5-136, and 4-136 atropisomers from different tissues are summarized in Table S12.

Quality Assurance/Quality Control. The ^{63}Ni-*μ*ECDs used for the PCB and HO-PCB analysis were linear up to concentrations of 1,000 ng/mL for all analytes investigated (R^2 > 0.999). A detailed summary of the limits of detection, limits of quantification, and background levels of PCB 136 and its metabolites is presented in Tables S5 and S6, Supporting Information. The recovery of PCB 117 and 4′-159 was 94 ± 7% (range: 84−102) and 95 ± 6% (range: 83−105), respectively. The average resolution[20] of PCB 136, 5-136, and 4-136 atropisomers on the enantioselective columns were 0.92 (BDM column or 0.87 (CB column), 0.69, and 0.75, respectively. The EF values for the racemic standards of PCB 136 on the BDM column and the CB column, 5-136 on the BDM column, and 4-136 on the CB column were 0.502 ± 0.001, 0.505 ± 0.004, 0.513 ± 0.016, and 0.499 ± 0.011, respectively. The EF values of PCB 136 determined on both enantioselective columns were not significantly different from each other (*t* test, $p > 0.05$).

Statistical Analyses. Unless otherwise stated, all data are reported as mean ± one standard deviation. Differences in biological measurements, tissue PCB and HO-PCB levels, and EF values between different treatment groups as well as differences of EF values from the respective racemic standard were tested with two-sample, two-tailed Student's *t* test. All differences were considered statistically significant for $p < 0.05$. Detailed results of the statistical analysis are provided in the Supporting Information.

RESULTS AND DISCUSSION

PCB 136 Tissue and Excreta Levels. KO mice had consistently higher PCB levels in tissues and excreta than WT mice, presumably due to defective hepatic PCB 136 metabolism. PCB 136 levels, expressed as percent of the total dose, decreased in the rank order adipose > liver > brain > blood in both WT and KO mice (Figure 2). The same rank order was observed when the PCB levels were adjusted for wet weight or extractable lipid content (Tables S7 and S9). The PCB 136 tissue distribution in WT mice was comparable to

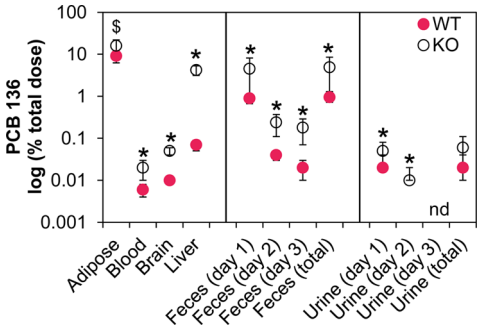

Figure 2. Female mice with defective hepatic metabolism due to liver-specific deletion of cytochrome P450 oxidoreductase (KO) have significantly higher levels of PCB 136 in tissues and feces compared to age-matched congenic wild type mice (WT). Data represent the mean ± standard deviation of the PCB 136 levels determined in the tissues and excreta of individual PCB l36-treated KO (n = 7) and WT mice (n = 5) and are expressed on a logarithmic scale as percent of the total PCB 136 dose (see Table S11 for additional details). * Significantly different from WT (t test, $p < 0.05$); $ different from WT (t test, $0.05 \leq p < 0.1$); nd, not detected.

similar studies in C57Bl/6 mice.[33,37−40] Feces and urine were minor routes of excretion of the parent compound. PCB 136 levels in feces and urine decreased from day 1 to day 3, which is also consistent with earlier PCB 136 disposition studies in rodents.[38,43,44]

Phenotypic differences in liver metabolism also contributed to higher PCB 136 levels in the liver and feces from KO versus congenic WT mice, thus resulting in a modest distribution of PCB 136 away from other organs, such as the brain; however, the overall effect of the higher liver and feces levels was small and, at most, slightly decreased systemic PCB 136 levels in KO mice. Consistent with previous studies, KO mice have larger livers as well as higher fat and P450 protein levels in the liver compared to congenic WT mice (Tables S1, S3, and S4).[31,45,46] The differences in the liver size and composition likely contribute to the retention of a considerable percentage of the total PCB 136 dose in the liver of KO versus WT mice (4.2% in KO versus 0.07% in WT mice, respectively). We also observed higher fecal lipid levels in KO compared to WT mice, which is likely due to a decreased absorption of fats caused by a lack of bile acid synthesis in KO mice.[46] Because systemic uptake, excretion, and reuptake of PCBs are driven by their lumen-to-tissue concentration gradient,[47,48] the higher gastrointestinal fat content in KO mice increased the fecal excretion PCB 136 levels in KO compared to WT mice. Specifically, 4.5% vs 1.0% of the total PCB 136 dose are excreted in the feces of KO and WT mice, respectively. An increased gastrointestinal fat content due to non-absorbable fats, such as Olestra, has also been shown to increase the fecal excretion of PCBs and other lipophilic pollutants in mice[49] and humans.[50]

HO-PCB Tissue Levels. Based on *in vitro* metabolism studies in different species, PCB 136 is metabolized by hepatic P450 enzymes to several hydroxylated metabolites, including 5-136, 4-136, and 3-150, a 1,2-shift metabolite of PCB 136 (Figure 1).[19−21,51,52] Both 5-136 and 4-136 can be further metabolized by P450 enzymes to a dihydroxylated metabolite, 4,5-136.[18,21] In agreement with these earlier metabolism studies, 5-136, 4-136, and 4,5-136 were detected in the liver, blood, and excreta from both KO and WT mice (Figure 3). 3-150 was a minor metabolite in the liver but was not detected in blood from KO and WT mice. All HO-PCB metabolites were

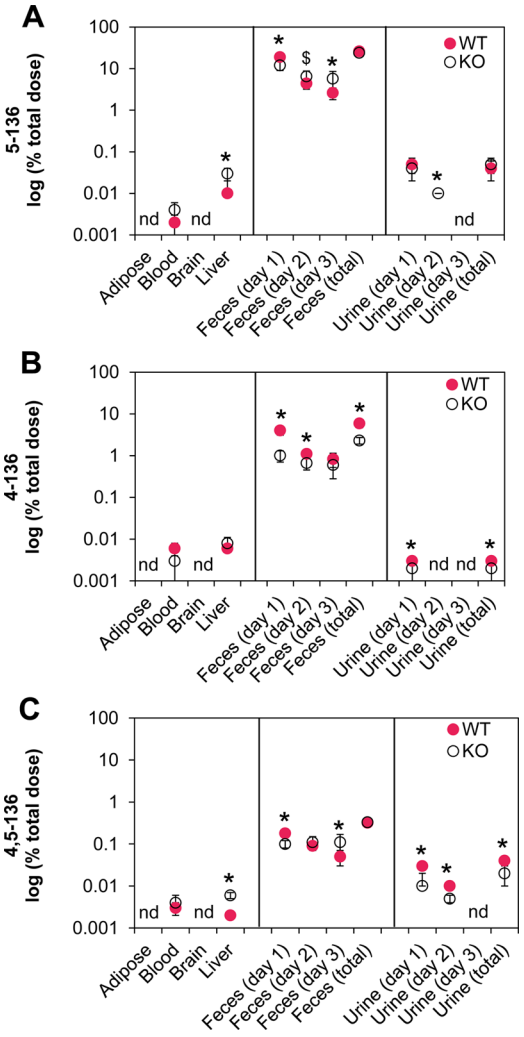

Figure 3. Comparison of the levels of (A) 5-136, (B) 4-136, and (C) 4,5-136 in tissues and excreta from female mice with defective hepatic metabolism (KO mice) and their age-matched congenic wild type mice (WT). PCB 136 is primarily eliminated as 5-136, and to a lesser extent as (B) 4-136 and (C) 4,5-136, in the feces of KO and WT mice; however, the time course of fecal HO-PCB metabolite and/or conjugate levels differ significantly between KO and WT mice. Data represent the mean ± standard deviation of the HO-PCB metabolites levels determined in the tissues and excreta of individual, PCB l36-treated KO (n = 7) and WT mice (n = 5) and are expressed on a logarithmic scale as percent of the total PCB 136 dose (see Table S11 for additional details). * Significantly different from WT (t test, $p < 0.05$); $ different from WT (t test, $0.05 \leq p < 0.1$); nd, not detected.

below the detection limit in adipose and brain tissue. In an earlier disposition study, we were also unable to detect HO-PCB metabolites of racemic PCB 95 in the brain of adult C57Bl/6 mice;[34] however, other studies have detected HO-PCBs in the brain of cetaceans,[53] polar bears,[54] and rats.[55] Other metabolites, including methylsulfone PCBs, PCB sulfates, and glucuronides were not analyzed in tissues because suitable analytical methods and standards are not available.

5-136, which is formed by rat, dog, and, likely, mouse CYP2B enzymes,[18−21] was the major metabolite in the liver from both KO and WT mice, with 5-136 levels being 3-fold higher in the liver of KO mice (Figure 3A). Livers from KO mice also contained higher levels of 4-136 and 4,5-136 compared to WT mice (Figures 3B and 3C), and a higher percentage of the total

dx.doi.org/10.1021/es504766p | Environ. Sci. Technol. 2015, 49, 616−625

PCB 136 dose were recovered as HO-PCBs from the liver of KO compared to WT mice (0.045% vs 0.018% of the total PCB 136 dose, respectively). In contrast to a PCB 95 disposition study,[34] HO-PCB levels in blood were typically lower compared to liver levels. Blood levels of 5-136 and 4,5-136 were higher in KO compared to WT mice (Figures 3A and 3C), whereas 4-136 levels were higher in WT compared to KO mice (Figure 3B). These differences between KO and WT mice were observed both for HO-PCB levels adjusted for wet weight or expressed as percent of the total PCB 136 dose (Tables S8 and S11). The higher HO-PCB levels in KO mice on day 3 are due to higher PCB 136 levels in KO mice and, consequently, result in the formation of more HO-PCB metabolites in KO than WT mice on day 3. Similarly, a toxicokinetics study with cyclophosphamide showed higher metabolite levels at certain time points due to the altered toxicokinetics in KO vs WT mice.[56]

HO-PCB Feces Levels. The levels of all HO-PCBs detected in feces decreased from day 1 to day 3 (Figure 3). Since the intestinal flora has glucuronidase and sulfatase activity,[57,58] it is unclear whether free HO-PCBs or the corresponding conjugates were eliminated via the bile into the feces. A recent study with 4-chlorobiphenyl (PCB 3) in rats suggests that HO-PCB conjugates were most likely eliminated into the feces, followed by their efficient deconjugation by the intestinal flora.[27] Interestingly, the time course of HO-PCB excretion differed between KO and WT mice, with fecal HO-PCB levels decreasing more rapidly in WT compared to KO mice (Figure 3). These differences in the time course of fecal HO-PCB excretion are consistent with a decreased hepatic PCB metabolism and, as a result, a higher internal PCB dose in KO mice.

Over the entire three-day study period, 32% and 27% of the total PCB 136 dose was recovered as HO-PCBs from the feces of WT and KO mice, respectively (Table S11). Similarly, a large percentage of PCB 136 was excreted as metabolites in the feces of senescent rats.[43] 5-136 was the major metabolite recovered from feces, with 26% and 24% of the total PCB 136 dose being excreted as 5-136 in the feces from WT and KO mice, respectively (Table S11). The high levels of 5-136 recovered from feces indicate a major role of CYP2B enzymes in the elimination of PCB 136 in mice. A smaller percentage of the total PCB 136 dose was recovered from feces as 4-136 (5.9% and 2.3% for WT and KO mice, respectively, Table S11). The large percentage of HO-PCBs recovered over the three day study period from feces of KO mice is surprising because, as we (see Table S1) and others[31] have shown, KO mice have essentially no hepatic CPR activity and, therefore, should not be able to metabolize PCB 136 in the liver; however, other xenobiotics, such as cyclophosphamide,[56] also undergo considerable biotransformation in KO mice. Extrahepatic metabolism of PCB 136 is the most likely explanation for the high fecal levels of HO-PCBs or their conjugates observed in our study. Indeed, P450 enzymes are expressed and functional in extrahepatic tissues in many organisms, including fish[59] and mammals.[60,61] For example, rat skin can metabolize PCB 136 *in vitro*.[62] However, we cannot completely rule out that liver cells other than hepatocytes metabolize PCBs in KO mice or that the cytochrome b_5 electron transfer pathway may support low levels of P450 enzyme activity, thus resulting in the formation of HO-PCBs.[56,63] Moreover, we cannot exclude the possibility that PCB 136 is differentially metabolized in KO vs WT by the gut microbiome.

HO-PCB Urine Levels. An earlier study in rats reported that urine was only a minor route of PCB 136 excretion, with most of the PCB 136 excreted as metabolites (>99%).[43] Recent studies of 4-chlorobiphenyl metabolism in rats suggest that these urinary metabolites are likely PCB conjugates.[27,64] Levels of HO-PCBs were, therefore, quantified in mouse urine with or without β-glucuronidase/sulfatase deconjugation to investigate if PCB conjugates are also excreted with the urine in mice. Urine was a minor route of excretion of HO-PCBs (Figure 3) and the corresponding sulfate and/or glucuronide conjugates (Figure 4), accounting for <0.2% of the total PCB 136 dose

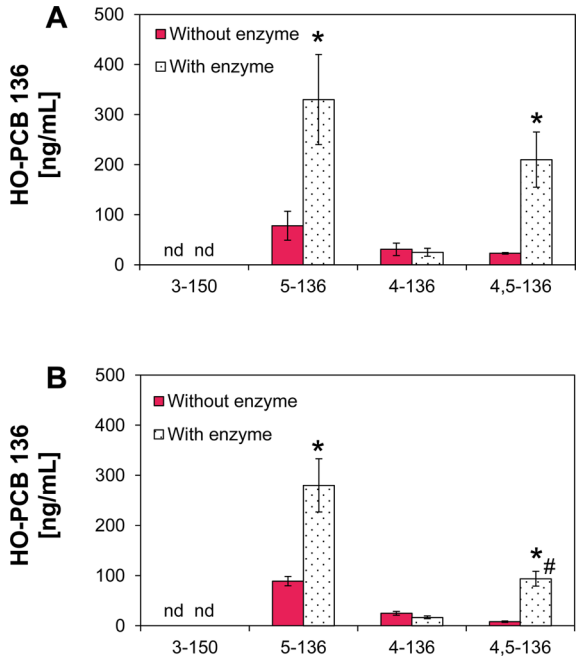

Figure 4. Treatment with β-glucuronidase/sulfatase significantly increased the levels of 5-136 and 4,5-136 in day 1 urine from (A) female wild type (WT) mice and (B) female mice with a liver-specific deletion of the cpr gene (KO), suggesting the presence of glucuronide and/or sulfate conjugates of both HO-PCBs in urine. Data represent the mean ± standard error of the mean of the HO-PCB metabolites levels determined in urine from individual, PCB l36-treated mice. *Significantly higher HO-PCB levels following deconjugation (*t* test, $p < 0.05$); # significantly higher 4,5-136 levels following deconjugation in WT mice compared to KO mice (*t* test, $p < 0.05$); nd, not detected.

(Table S11). After deconjugation, 5-136, 4-136, and 4,5-136, but not 3-150, were detected in day 1 and, to some extent, day 2 urine samples (Figure 3). No HO-PCB metabolites were detected in day 3 urine samples. β-Glucuronidase/sulfatase treatment significantly increased urinary 5-136 and 4,5-136 but not 4-136 levels in urine samples (Figure 4), which demonstrates that some HO-PCB 136 metabolites, such as 5-136 and 4,5-136, are further metabolized to the corresponding sulfate and/or glucuronide conjugates in mice. There is growing evidence that sulfate conjugates of HO-PCBs in particular are important metabolites formed by plants,[65] wildlife,[25,26] or laboratory animals.[27] Further studies are needed to further characterize the conjugates, their chiral signatures, and assess their role in PCB developmental neurotoxicity in wildlife and laboratory animals.

Enantiomeric Fractions of PCB 136 in Tissues and Excreta. The enantiomeric fractions of PCB 136 were determined to assess whether decreased hepatic metabolism

dx.doi.org/10.1021/es504766p | *Environ. Sci. Technol.* 2015, 49, 616−625

alters the atropselective disposition and excretion of PCB 136. In both KO and WT mice, the EF values of PCB 136 were >0.5 in all tissues and excreta investigated, with EF values significantly different from the racemic standards (t test, $p < 0.05$) (Figure 5). This direction of atropisomeric enrichment is consistent with the enrichment of (+)-PCB 136 reported previously for mice.[33,37−40] The most pronounced atropisomeric enrichment was observed in liver samples, with EF values of 0.70 and 0.74 in KO and WT mice, respectively. EF values decreased in the order liver > blood ∼ brain > adipose. Several other disposition studies have also reported the most pronounced atropisomeric enrichment of PCB 136 in liver and a less pronounced enrichment in adipose tissue.[33,39] Interestingly, the EF values of PCB 136 in different tissues were by and large not significantly different between KO and WT mice (Table S12), i.e., reduced hepatic PCB metabolism did not alter the chiral signature of PCB 136 in the mouse, at least at the time point investigated. Vice versa, increased hepatic PCB metabolism due to the induction of CYP2B enzymes with phenobarbital also had no significant effect on chiral PCB 136 signatures in mice.[39] Because extrahepatic P450 enzyme activities are probably not affected by the liver-specific deletion of the *cpr* gene (this study) or phenobarbital treatment,[39] a contribution of extrahepatic metabolism to the biotransformation of PCB 136 may explain why changes in the metabolic capacity of the liver have no clear effect on chiral signatures in mice; however, additional studies are needed to further explore this hypothesis.

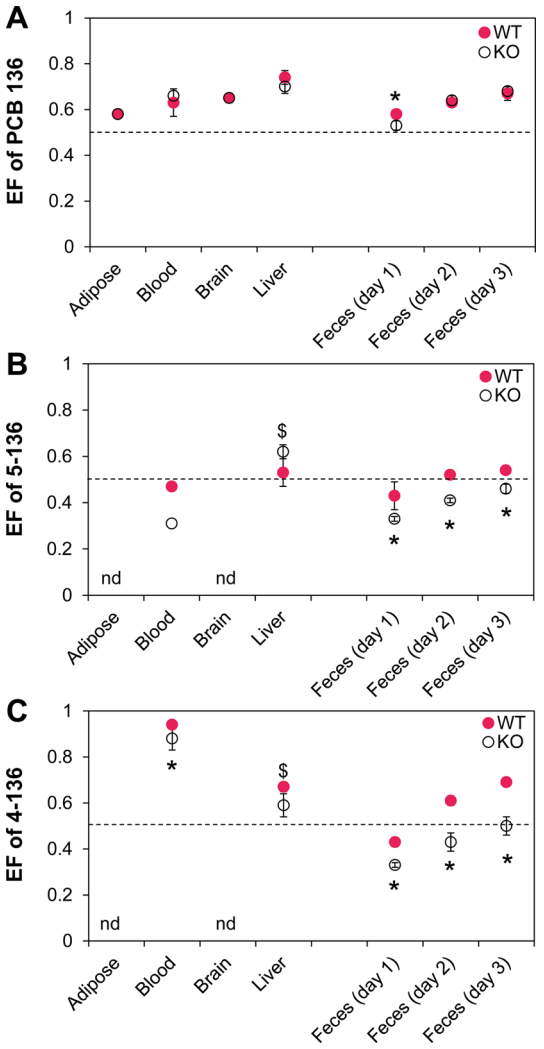

Figure 5. Comparison of the enantiomeric fractions (EFs) of PCB 136 (A), 5-136 (B), and 4-136 (C) in tissues and feces reveals significant differences in the atropisomeric enrichment between female mice with a liver-specific deletion of the *cpr* gene (KO) and congenic wild type (WT) mice. The EF values are presented as the mean ± standard deviation and were determined in the tissues of individual PCB 136-treated KO ($n = 7$) and WT mice ($n = 5$). The only exceptions are the EF determination for 5-136 in blood, which were performed with a single sample pooled by genotype. A CB column was used to separated PCB 136 and 4-136, whereas a BDM column was used for separation of 5-136 (see Table S12 for additional details). * Significantly different from WT (t test, $p < 0.05$); $ different from WT (t test, $0.05 \leq p < 0.1$); nd, not detected; the dotted line indicates the EF values of the respective racemic standard.

Enantiomeric Fractions of HO-PCB 136 Metabolites in Tissues. Several recent studies have reported that hydroxylated metabolites of chiral PCBs are formed atropselectively in mice.[19,34] In agreement with these earlier studies, 5-136 and 4-136 displayed atropisomeric enrichment in tissues and excreta from both KO and WT mice. Remarkably, the extent and direction of the enrichment was different between KO and WT mice (Figures 5B and 5C). E_2-5-136 was enriched in the liver of KO mice, whereas 5-136 was near racemic in liver samples from WT mice (Figure 5B); however, the difference in the EF values between KO and WT mice in the liver did not reach statistical significance (t test, p = 0.058). In contrast, analysis of pooled blood samples revealed an atropisomeric enrichment of E_1-5-136 in the blood from KO mice. A much less pronounced enantiomeric enrichment of E_1-5-136 was present in pooled blood samples from WT animals. E_2-4-136 was enriched in blood and liver samples of KO and WT mice (Figure 5C), with WT mice displaying a more pronounced atropisomeric enrichment in blood and liver compared to KO mice.

Interestingly, the direction of the atropisomeric enrichment of HO-PCBs in the liver was different compared to the enrichment observed in *in vitro* metabolism studies. While E_2-5-136 and E_2-4-136 were typically enriched in the liver from KO and WT mice, E_1-5-136 and E_1-4-136 were preferentially formed in studies using mouse liver microsomes[52] and tissue slices.[19] In contrast, *in vitro* models generally predict the direction of the atropisomeric enrichment of the parent PCB *in vivo*, which is consistent with a major role of P450 enzymes in the atropisomeric enrichment of PCBs *in vivo*. It is therefore likely that, in addition to their atropselective formation by P450 enzymes, other processes play a role in the atropselective disposition of HO-PCB metabolites.

Enantiomeric Fractions of HO-PCB 136 Metabolites in Excreta. The EF values of 5-136 and 4-136 in feces samples changed over time (Figures 5B and 5C). E_1-5-136 and E_1-4-136 were enriched in day 1 feces samples from both KO and WT mice, with KO mice displaying significantly more pronounced atropisomeric enrichment compared to WT mice. EF values of both 5-136 and 4-136 changed from day 1 to day 3 feces samples, with EF values in KO mice always being significantly smaller compared to WT mice. In KO mice, E_1-5-136 and E_1-4-136 were enriched in day 2 feces samples, whereas both metabolites were near racemic in day 3 feces samples. In contrast, 5-136 was near racemic and E_2-4-136 was enriched in day 2 and day 3 feces samples from WT mice. EF values of HO-PCB could only be determined in day 1 urine samples. Consistent with day 1 feces samples, pooled day 1 urine

dx.doi.org/10.1021/es504766p | *Environ. Sci. Technol.* 2015, 49, 616−625

samples also displayed an enrichment of E_1-5-136 and E_1-4-136 (Table S12).

Differences in the subsequent atropselective phase II metabolism of HO-PCBs as well as the active transport of HO-PCBs and their glucuronide or sulfate conjugates are one possible explanation for these differences. For example, we have shown that HO-PCBs are atropselectively oxidized to dihydroxylated metabolites.[18] Moreover, differences in the atropselective biotransformation of HO-PCB 136 metabolites to sulfate and/or glucuronide conjugates may contribute to the differences in the chiral HO-PCB signatures between WT and KO mice. Indeed, earlier studies have demonstrated the compensatory induction of various drug metabolizing enzymes (e.g., glucuronosyltransferases) in KO mice.[45,46] In addition to phase II metabolism, differences in the atropselective active transport of the HO-PCB and/or their conjugates may explain why the extent and direction of the atropisomeric enrichment of the HO-PCB metabolites in feces samples changed over time and differed between KO and WT mice. Further studies to understand the atropselective disposition of PCB metabolites are therefore needed in terrestrial and aquatic organisms, especially considering the fact that HO-PCB and, possibly their conjugates, are also toxic.

Environmental Relevance. To date, most PCB metabolism studies have focused on mammalian P450 enzymes;[18,20−23,52] however, there is growing evidence that P450 enzymes contribute to the biotransformation of PCBs in plants,[66−69] fish,[10,59,70,71] birds,[72] and marine mammals.[73] As suggested by our results, it is likely that hepatic and possibly extrahepatic metabolism by P450 enzymes plays a major role in the biotransformation of PCBs and structurally related compounds in wildlife, laboratory animals, and humans and contributes to the atropisomeric enrichment of PCBs observed in wildlife.[24] Moreover, HO-PCBs can undergo phase II biotransformation to glucuronides and sulfates in laboratory animal models[27] and in environmentally relevant species, such as polar bear.[25,26] Our findings in mice suggest that, in addition to P450 enzymes, phase II biotransformation represents a currently unexplored factor in the atropselective disposition of chiral HO-PCB. Further understanding these biotransformation processes is important because HO-PCBs are potentially toxic and contribute to the adverse effects of PCBs in the environment and in humans. Since animal models with a deletion or knockdown of genes of key enzymes involved in PCB biotransformation (e.g., *cpr* or P450 enzymes) can be generated for various species, including fish[74,75] and mice,[31,32] such models are powerful tools to explore the importance of hepatic vs extrahepatic metabolism in PCB disposition in wildlife and laboratory animals. Furthermore, these types of models may be useful for studying how metabolism modulates the developmental neurotoxicity of PCBs and other environmental contaminants. The feasibility of such studies is indicated by our observation that genetic deletion of *cpr* in the liver does not significantly alter neurodevelopment as determined by an assessment of synaptic plasticity genes in the brains of KO vs WT mice (Table S2).

■ ASSOCIATED CONTENT

Supporting Information

Characterization of the mouse model (i.e., hepatic enzyme levels and activities; transcript levels of synaptic plasticity genes in different brain regions); body and organ weights of PCB 136 or vehicle-treated female WT and KO mice; extractable lipid content expressed as percent of tissue or feces wet weight in PCB 136 or vehicle-treated WT and KO mice; limits of detection *(LODs)*, limits of quantification *(LOQs)*, and background levels of PCB 136 and HO-PCB 136 metabolites in tissues and excreta from vehicle-treated mice; wet weight and lipid adjusted concentrations of PCB 136 and HO-PCB 136 metabolites in tissues and excreta; amount of PCB 136 and HO-PCB 136 metabolites in tissues and excreta expressed as percent of the total PCB 136 dose; and a comparison of the enantiomeric fraction (EF) of the PCB 136, 5-136, and 4-136 in tissues and excreta. This material is available free of charge via the Internet at http://pubs.acs.org.

■ AUTHOR INFORMATION

Corresponding Author

*Phone: 319 335-4310. Fax: 319 335-4290. E-mail: hans-joachim-lehmler@uiowa.edu. Corresponding author address: Department of Occupational and Environmental Health, The University of Iowa, University of Iowa Research Park, #221 IREH, Iowa City, IA 52242-5000.

Funding

This work was supported by grants ES05605, ES013661, and ES017425 from the National Institute of Environmental Health Sciences, National Institutes of Health. The synthesis of several hydroxylated PCB 136 standards was funded by NIH grant ES06694. The content is solely the responsibility of the authors and does not necessarily represent the official views of the National Institute of Environmental Health Sciences or the National Institutes of Health.

Notes

The authors declare no competing financial interest.

■ ACKNOWLEDGMENTS

The authors would like to thank Dr. Xinxin Ding of the Wadsworth Center, New York State Department of Health, for providing the mouse model, Dr. E. Davis Oldham for help with the animal work, Austin Kammerer for help with the PCB analysis, and Dr. Izabela Kania-Korwel for technical support and a critical review of the manuscript. The PCB 136 derivatives were a generous gift from E. A. Mash and S. C. Waller of the Synthetic Chemistry Facility Core of the Southwest Environmental Health Sciences Center.

■ REFERENCES

(1) Stockholm Convention on Persistent Organic Pollutants (PCBs overview). http://chm.pops.int/Implementation/PCBs/Overview/tabid/273/Default.aspx (accessed 11/19/2014).

(2) Jamshidi, A.; Hunter, S.; Hazrati, S.; Harrad, S. Concentrations and chiral signatures of polychlorinated biphenyls in indoor and outdoor air and soil in a major UK conurbation. *Environ. Sci. Technol.* **2007**, *41*, 2153−2158.

(3) Zheng, J.; Yan, X.; Chen, S. J.; Peng, X. W.; Hu, G. C.; Chen, K. H.; Luo, X. J.; Mai, B. X.; Yang, Z. Y. Polychlorinated biphenyls in human hair at an e-waste site in China: composition profiles and chiral signatures in comparison to dust. *Environ. Int.* **2013**, *54*, 128−133.

(4) Tue, N. M.; Takahashi, S.; Suzuki, G.; Isobe, T.; Viet, P. H.; Kobara, Y.; Seike, N.; Zhang, G.; Sudaryanto, A.; Tanabe, S. Contamination of indoor dust and air by polychlorinated biphenyls and brominated flame retardants and relevance of non-dietary exposure in Vietnamese informal e-waste recycling sites. *Environ. Int.* **2013**, *51*, 160−167.

(5) Chen, S. J.; Tian, M.; Zheng, J.; Zhu, Z. C.; Luo, Y.; Luo, X. J.; Mai, B. X. Elevated levels of polychlorinated biphenyls in plants, air, and soils at an e-waste site in Southern China and enantioselective

biotransformation of chiral PCBs in plants. *Environ. Sci. Technol.* **2014**, *48*, 3847−3855.
(6) Hu, D.; Hornbuckle, K. C. Inadvertent polychlorinated biphenyls in commercial paint pigments. *Environ. Sci. Technol.* **2010**, *44*, 2822−2827.
(7) Anezaki, K.; Nakano, T. Concentration levels and congener profiles of polychlorinated biphenyls, pentachlorobenzene, and hexachlorobenzene in commercial pigments. *Environ. Sci. Pollut. Res.* **2013**, 1−12.
(8) Thomas, K.; Xue, J.; Williams, R.; Jones, P.; Whitaker, D. United States Environmental Protection Agency, Office of Research and Development, National Exposure Research Laboratory (2012) Polychlorinated biphenyls (PCBs) in school buildings: Sources, environmental levels, and exposures. http://www.epa.gov/wastes/hazard/tsd/pcbs/pubs/caulk/pdf/pcb_EPA600R12051_final.pdf. (accessed 11/19/2014).
(9) Kostyniak, P.; Hansen, L.; Widholm, J.; Fitzpatrick, R.; Olson, J.; Helferich, J.; Kim, K.; Sable, H.; Seegal, R.; Pessah, I.; Schantz, S. Formulation and characterization of an experimental PCB mixture designed to mimic human exposure from contaminated fish. *Toxicol. Sci.* **2005**, *88*, 400−411.
(10) Lu, Z.; Fisk, A. T.; Kovacs, K. M.; Lydersen, C.; McKinney, M. A.; Tomy, G. T.; Rosenburg, B.; McMeans, B. C.; Muir, D. C.; Wong, C. S. Temporal and spatial variation in polychlorinated biphenyl chiral signatures of the Greenland shark (*Somniosus microcephalus*) and its arctic marine food web. *Environ. Pollut.* **2014**, *186*, 216−225.
(11) Mitchell, M. M.; Woods, R.; Chi, L. H.; Schmidt, R. J.; Pessah, I. N.; Kostyniak, P. J.; LaSalle, J. M. Levels of select PCB and PBDE congeners in human postmortem brain reveal possible environmental involvement in 15q11-q13 duplication autism spectrum disorder. *Environ. Mol. Mutagen.* **2012**, *53*, 589−598.
(12) Megson, D.; O'Sullivan, G.; Comber, S.; Worsfold, P. J.; Lohan, M. C.; Edwards, M. R.; Shields, W. J.; Sandau, C. D.; Patterson, D. G. J. Elucidating the structural properties that influence the persistence of PCBs in humans using the National Health and Nutrition Examination Survey (NHANES) dataset. *Sci. Total Environ.* **2013**, *461−462C*, 99−107.
(13) DeCaprio, A. P.; Johnson, G. W.; Tarbell, A. M.; Carpenter, D. O.; Chiarenzelli, J. R.; Morse, G. S.; Santiago-Rivera, A. L.; Schymura, M. J. Polychlorinated biphenyl (PCB) exposure assessment by multivariate statistical analysis of serum congener profiles in an adult Native American population. *Environ. Res.* **2005**, *98*, 284−302.
(14) Hamers, T.; Kamstra, J. H.; Cenijn, P. H.; Pencikova, K.; Palkova, L.; Simeckova, P.; Vondracek, J.; Andersson, P. L.; Stenberg, M.; Machala, M. In vitro toxicity profiling of ultrapure non−dioxin-like polychlorinated biphenyl congeners and their relative toxic contribution to PCB mixtures in humans. *Toxicol. Sci.* **2011**, *121*, 88−100.
(15) Mariussen, E.; Fonnum, F. Neurochemical targets and behavioral effects of organohalogen compounds: an update. *Crit. Rev. Toxicol.* **2006**, *36*, 253−289.
(16) Pessah, I. N.; Cherednichenko, G.; Lein, P. J. Minding the calcium store: Ryanodine receptor activation as a convergent mechanism of PCB toxicity. *Pharmacol. Ther.* **2010**, *125*, 260−285.
(17) Fritsch, E. B.; Pessah, I. N. Structure-activity relationship of non-coplanar polychlorinated biphenyls toward skeletal muscle ryanodine receptors in rainbow trout (*Oncorhynchus mykiss*). *Aquat. Toxicol.* **2013**, *140−141*, 204−212.
(18) Lu, Z.; Kania-Korwel, I.; Lehmler, H.-J.; Wong, C. S. Stereoselective formation of mono- and di-hydroxylated polychlorinated biphenyls by rat cytochrome P450 2B1. *Environ. Sci. Technol.* **2013**, *47*, 12184−12192.
(19) Wu, X.; Duffel, M. W.; Lehmler, H.-J. Oxidation of polychlorinated biphenyls by liver tissue slices from phenobarbital-pretreated mice is congener-specific and atropselective. *Chem. Res. Toxicol.* **2013**, *26*, 1642−1651.
(20) Wu, X.; Pramanik, A.; Duffel, M. W.; Hrycay, E. G.; Bandiera, S. M.; Lehmler, H. J.; Kania-Korwel, I. 2,2′,3,3′,6,6′-Hexachlorobiphenyl (PCB 136) is enantioselectively metabolized to hydroxylated metabolites by rat liver microsomes. *Chem. Res. Toxicol.* **2011**, *24*, 2249−2257.
(21) Waller, S. C.; He, Y. A.; Harlow, G. R.; He, Y. Q.; Mash, E. A.; Halpert, J. R. 2,2′,3,3′,6,6′-Hexachlorobiphenyl hydroxylation by active site mutants of cytochrome P450 2B1 and 2B11. *Chem. Res. Toxicol.* **1999**, *12*, 690−699.
(22) Warner, N. A.; Martin, J. W.; Wong, C. S. Chiral polychlorinated biphenyls are biotransformed enantioselectively by mammalian cytochrome P-450 isozymes to form hydroxylated metabolites. *Environ. Sci. Technol.* **2009**, *43*, 114−121.
(23) Kennedy, M. W.; Carpentier, N. K.; Dymerski, P. P.; Kaminsky, L. S. Metabolism of dichlorobiphenyls by hepatic microsomal cytochrome P-450. *Biochem. Pharmacol.* **1981**, *30*, 577−588.
(24) Lehmler, H.-J.; Harrad, S. J.; Hühnerfuss, H.; Kania-Korwel, I.; Lee, C. M.; Lu, Z.; Wong, C. S. Chiral polychlorinated biphenyl transport, metabolism, and distribution: A review. *Environ. Sci. Technol.* **2010**, *44*, 2757−2766.
(25) Sacco, J. C.; James, M. O. Glucuronidation in the polar bear (Ursus maritimus). *Mar. Environ. Res.* **2004**, *58*, 475−479.
(26) Sacco, J. C.; James, M. O. Sulfonation of environmental chemicals and their metabolites in the polar bear (*Ursus maritimus*). *Drug Metab. Dispos.* **2005**, *33*, 1341−1348.
(27) Dhakal, K.; Uwimana, E.; Adamcakova-Dodd, A.; Thorne, P. S.; Lehmler, H. J.; Robertson, L. W. Disposition of phenolic and sulfated metabolites after inhalation exposure to 4-chlorobiphenyl (PCB3) in female rats. *Chem. Res. Toxicol.* **2014**, *27*, 1411−1420 DOI: DOI: 10.1021/tx500150h.
(28) Yang, D.; Kania-Korwel, I.; Ghogha, A.; Chen, H.; Stamou, M.; Bose, D. D.; Pessah, I. N.; Lehmler, H. J.; Lein, P. J. PCB 136 atropselectively alters morphometric and functional parameters of neuronal connectivity in cultured rat hippocampal neurons via ryanodine receptor-dependent mechanisms. *Toxicol. Sci.* **2014**, *138*, 379−392.
(29) Kania-Korwel, I.; Vyas, S.; Song, Y.; Lehmler, H. J. Gas chromatographic separation of methoxylated polychlorinated biphenyl atropisomers. *J. Chromatogr. A* **2008**, *1207*, 146−154.
(30) Black, T. H. The preparation and reactions of diazomethane. *Aldrichimica Acta* **1982**, *15*, 3−10.
(31) Gu, J.; Weng, Y.; Zhang, Q. Y.; Cui, H.; Behr, M.; Wu, L.; Yang, W.; Zhang, L.; Ding, X. Liver-specific deletion of the NADPH-cytochrome P450 reductase gene: impact on plasma cholesterol homeostasis and the function and regulation of microsomal cytochrome P450 and heme oxygenase. *J. Biol. Chem.* **2003**, *278*, 25895−25901.
(32) Wu, L.; Gu, J.; Weng, Y.; Kluetzman, K.; Swiatek, P.; Behr, M.; Zhang, Q. Y.; Zhuo, X.; Xie, Q.; Ding, X. Conditional knockout of the mouse NADPH-cytochrome p450 reductase gene. *Genesis* **2003**, *36*, 177−181.
(33) Kania-Korwel, I.; Shaikh, N.; Hornbuckle, K. C.; Robertson, L. W.; Lehmler, H.-J. Enantioselective disposition of PCB 136 (2,2′,3,3′,6,6′-hexachlorobiphenyl) in C57BL/6 mice after oral and intraperitoneal administration. *Chirality* **2007**, *19*, 56−66.
(34) Kania-Korwel, I.; Barnhart, C. D.; Stamou, M.; Truong, K. M.; El-Komy, M. H.; Lein, P. J.; Veng-Pedersen, P.; Lehmler, H. J. 2,2′,3,5′,6-Pentachlorobiphenyl (PCB 95) and its hydroxylated metabolites are enantiomerically enriched in female mice. *Environ. Sci. Technol.* **2012**, *46*, 11393−11401.
(35) Wu, X.; Murphy, P.; Cunnick, J.; Hendrich, S. Synthesis and characterization of deoxynivalenol glucuronide: its comparative immunotoxicity with deoxynivalenol. *Food Chem. Toxicol.* **2007**, *45*, 1846−1855.
(36) Wu, X.; Kania-Korwel, I.; Chen, H.; Stamou, M.; Dammanahalli, K.; Duffel, M.; Lein, P. J.; Lehmler, H.-J. Metabolism of 2,2′,3,3′,6,6′-hexachlorobiphenyl (PCB 136) atropisomers in tissue slices from phenobarbital or dexamethasone-induced rats is sex-dependent. *Xenobiotica* **2013**, *43*, 933−947.
(37) Milanowski, B.; Lulek, J.; Lehmler, H.-J.; Kania-Korwel, I. Assessment of the disposition of chiral polychlorinated biphenyls in

female mdr 1a/b knockout versus wild-type mice using multivariate analyses. *Environ. Int.* **2010**, *36*, 884−892.
(38) Kania-Korwel, I.; Hornbuckle, K. C.; Robertson, L. W.; Lehmler, H.-J. Influence of dietary fat on the enantioselective disposition of 2,2′,3,3′,6,6′-hexachlorobiphenyl (PCB 136) in female mice. *Food Chem. Toxicol.* **2008**, *46*, 637−644.
(39) Kania-Korwel, I.; Xie, W.; Hornbuckle, K. C.; Robertson, L. W.; Lehmler, H.-J. Enantiomeric enrichment of 2,2′,3,3′,6,6′-hexachlorobiphenyl (PCB 136) in mice after induction of CYP enzymes. *Arch. Environ. Contam. Toxicol.* **2008**, *55*, 510−517.
(40) Kania-Korwel, I.; Hornbuckle, K. C.; Robertson, L. W.; Lehmler, H.-J. Dose-dependent enantiomeric enrichment of 2,2′,3,3′,6,6′-hexachlorobiphenyl in female mice. *Environ. Toxicol. Chem.* **2008**, *27*, 299−305.
(41) Kania-Korwel, I.; Lehmler, H. J. Assigning atropisomer elution orders using atropisomerically enriched polychlorinated biphenyl fractions generated by microsomal metabolism. *J. Chromatogr. A* **2013**, *1278*, 133−144.
(42) Haglund, P.; Wiberg, K. Determination of the gas chromatographic elution sequences of the (+) and (−) enantiomers of stable enantiomeric PCBs on Chirasil-Dex. *J. High Resol. Chromatogr.* **1996**, *19*, 373−376.
(43) Birnbaum, L. S. Distribution and excretion of 2,3,6,2′,3′,6′- and 2,4,5,2′,4′,5′-hexachlorobiphenyl in senescent rats. *Toxicol. Appl. Pharmacol.* **1983**, *3*, 262−272.
(44) Sipes, I.; Slocumb, M.; Perry, D.; Carter, D. 2,4,5,2′,4′,5′-Hexachlorobiphenyl: distribution, metabolism, and excretion in the dog and the monkey. *Toxicol. Appl. Pharma.* **1982**, *65*, 264−272.
(45) Gu, J.; Cui, H.; Behr, M.; Zhang, L.; Zhang, Q. Y.; Yang, W.; Hinson, J. A.; Ding, X. In vivo mechanisms of tissue-selective drug toxicity: effects of liver-specific knockout of the NADPH-cytochrome P450 reductase gene on acetaminophen toxicity in kidney, lung, and nasal mucosa. *Mol. Pharmacol.* **2005**, *67*, 623−630.
(46) Weng, Y.; DiRusso, C. C.; Reilly, A. A.; Black, P. N.; Ding, X. Hepatic gene expression changes in mouse models with liver-specific deletion or global suppression of the NADPH-cytochrome P450 reductase gene. Mechanistic implications for the regulation of microsomal cytochrome P450 and the fatty liver phenotype. *J. Biol. Chem.* **2005**, *280*, 31686−31698.
(47) Gobas, F. A. P. C.; McCorquodale, J. R.; Haffner, G. D. Intestinal absorption and biomagnification of organochlorines. *Environ. Toxicol. Chem.* **1993**, *12*, 567−576.
(48) Dulfer, W. J.; Groten, J. P.; Govers, H. A. Effect of fatty acids and the aqueous diffusion barrier on the uptake and transport of polychlorinated biphenyls in Caco-2 cells. *J. Lipid Res.* **1996**, *37*, 950−961.
(49) Jandacek, R.; Anderson, N.; Liu, M.; Zheng, S.; Yang, Q.; Tso, P. Effects of yo-yo diet, caloric restriction, and olestra on tissue distribution of hexachlorobenzene. *Am. J. Physiol.: Gastrointest. Liver Physiol.* **2005**, *288*, G292−299.
(50) Redgrave, T.; Wallace, P.; Jandacek, R.; Tso, P. Treatment with a dietary fat substitute decreased Arochlor 1254 contamination in an obese diabetic male. *J. Nutr. Biochem.* **2005**, *16*, 383−384.
(51) Schnellmann, R.; Putnam, C.; Sipes, I. Metabolism of 2,2′,3,3′,6,6′-hexachlorobiphenyl and 2,2′,4,4′,5,5′-hexachlorobiphenyl by human hepatic microsomes. *Biochem. Pharmacol.* **1983**, *32*, 3233−3239.
(52) Wu, X.; Kammerer, A.; Lehmler, H. J. Microsomal oxidation of 2,2′,3,3′,6,6′-hexachlorobiphenyl (PCB 136) results in species-dependent chiral signatures of the hydroxylated metabolites. *Environ. Sci. Technol.* **2014**, *48*, 2436−2444.
(53) Kunisue, T.; Sakiyama, T.; Yamada, T. K.; Takahashi, S.; Tanabe, S. Occurrence of hydroxylated polychlorinated biphenyls in the brain of cetaceans stranded along the Japanese coast. *Mar. Pollut. Bull.* **2007**, *54*, 963−973.
(54) Gebbink, W. A.; Sonne, C.; Dietz, R.; Kirkegaard, M.; Riget, F. F.; Born, E. W.; Muir, D. C.; Letcher, R. J. Tissue-specific congener composition of organohalogen and metabolite contaminants in East Greenland polar bears (Ursus maritimus). *Environ. Pollut.* **2008**, *152*, 621−629.
(55) Meerts, I. A.; Assink, Y.; Cenijn, P. H.; Van Den Berg, J. H.; Weijers, B. M.; Bergman, A.; Koeman, J. H.; Brouwer, A. Placental transfer of a hydroxylated polychlorinated biphenyl and effects on fetal and maternal thyroid hormone homeostasis in the rat. *Toxicol. Sci.* **2002**, *68*, 361−371.
(56) Pass, G. J.; Carrie, D.; Boylan, M.; Lorimore, S.; Wright, E.; Houston, B.; Henderson, C. J.; Wolf, C. R. Role of hepatic cytochrome P450s in the pharmacokinetics and toxicity of cyclophosphamide: studies with the hepatic cytochrome P450 reductase null mouse. *Cancer Res.* **2005**, *65*, 4211−4217.
(57) Asano, Y.; Hiramoto, T.; Nishino, R.; Aiba, Y.; Kimura, T.; Yoshihara, K.; Koga, Y.; Sudo, N. Critical role of gut microbiota in the production of biologically active, free catecholamines in the gut lumen of mice. *Am. J. Physiol.: Gastrointest. Liver Physiol.* **2012**, *303*, G1288−1295.
(58) Gloux, K.; Berteau, O.; El Oumami, H.; Béguet, F.; Leclerc, M.; Doré, J. A metagenomic β-glucuronidase uncovers a core adaptive function of the human intestinal microbiome. *Proc. Natl. Acad. Sci. U. S. A.* **2011**, *108* (Suppl), 4539−4546.
(59) Goldstone, J.; McArthur, A.; Kubota, A.; Zanette, J.; Parente, T.; Jonsson, M.; Nelson, D.; Stegeman, J. Identification and developmental expression of the full complement of cytochrome P450 genes in zebrafish. *BMC Genomics* **2010**, *11*, 643.
(60) Ding, X.; Kaminsky, L. S. Human extrahepatic cytochromes P450: Function in xenobiotic metabolism and tissue-selective chemical toxicity in the respiratory and gastrointestinal tracts. *Annu. Rev. Pharmacol. Toxicol.* **2003**, *43*, 149−173.
(61) Renaud, H. J.; Cui, J. Y.; Khan, M.; Klaassen, C. D. Tissue distribution and gender-divergent expression of 78 cytochrome P450 mRNAs in mice. *Toxicol. Sci.* **2011**, *124*, 261−277.
(62) Garner, C. E.; Demeter, J.; Matthews, H. B. The effect of chlorine substitution on the disposition of polychlorinated biphenyls following dermal administration. *Toxicol. Appl. Pharmacol.* **2006**, *216*, 157−167.
(63) Li, L.; Porter, T. D. Chlorzoxazone hydroxylation in microsomes and hepatocytes from cytochrome P450 oxidoreductase-null mice. *J. Biochem. Mol. Toxicol.* **2009**, *23*, 357−363.
(64) Dhakal, K.; He, X.; Lehmler, H. J.; Teesch, L. M.; Duffel, M. W.; Robertson, L. W. Identification of sulfated metabolites of 4-chlorobiphenyl (PCB3) in the serum and urine of male rats. *Chem. Res. Toxicol.* **2012**, *25*, 2796−2804.
(65) Zhai, G.; Lehmler, H. J.; Schnoor, J. L. Sulfate metabolites of 4-monochlorobiphenyl in whole poplar plants. *Environ. Sci. Technol.* **2013**, *47*, 557−562.
(66) Zhai, G.; Hu, D.; Lehmler, H. J.; Schnoor, J. L. Enantioselective biotransformation of chiral PCBs in whole poplar plants. *Environ. Sci. Technol.* **2011**, *45*, 2308−2316.
(67) Zhai, G.; Lehmler, H. J.; Schnoor, J. L. Hydroxylated metabolites of 4-monochlorobiphenyl and its metabolic pathway in whole poplar plants. *Environ. Sci. Technol.* **2010**, *44*, 3901−3907.
(68) Zhai, G.; Lehmler, H. J.; Schnoor, J. L. Inhibition of cytochromes P450 and the hydroxylation of 4-monochlorobiphenyl in whole poplar. *Environ. Sci. Technol.* **2013**, *47*, 6829−6835.
(69) Dai, S.; Wong, C. S.; Qiu, J.; Wang, M.; Chai, T.; Fan, L.; Yang, S. Enantioselective accumulation of chiral polychlorinated biphenyls in lotus plant (*Nelumbonucifera spp.*). *J. Hazard. Mater.* **2014**, *280*, 612−618.
(70) Buckman, A. H.; Brown, S. B.; Small, J.; Muir, D. C. G.; Parrott, J.; Solomon, K. R.; Fisk, A. T. Role of temperature and enzyme induction in the biotransformation of polychlorinated biphenyls and bioformation of hydroxylated polychlorinated biphenyls by rainbow trout (*Oncorhynchus mykiss*). *Environ. Sci. Technol.* **2007**, *41*, 3856−3863.
(71) Buckman, A. H.; Wong, C. S.; Chow, E. A.; Brown, S. B.; Solomon, K. R.; Fisk, A. T. Biotransformation of polychlorinated biphenyls (PCBs) and bioformation of hydroxylated PCBs in fish. *Aquat. Toxicol.* **2006**, *78*, 176−185.

(72) Borlakoglu, J. T.; Wilkins, J. P. Metabolism of di-, tri-, tetra-, penta- and hexachlorobiphenyls by hepatic microsomes isolated from control animals and animals treated with Aroclor 1254, a commercial mixture of polychlorinated biphenyls (PCBs). *Comp. Biochem. Physiol., Part C: Pharmacol., Toxicol. Endocrinol.* **1993**, *105*, 95−106.
(73) McKinney, M. A.; De Guise, S.; Martineau, D.; Béland, P.; Arukwe, A.; Letcher, R. J. Biotransformation of polybrominated diphenyl ethers and polychlorinated biphenyls in beluga whale (*Delphinapterus leucas*) and rat mammalian model using an in vitro hepatic microsomal assay. *Aquat. Toxicol.* **2006**, *77*, 87−97.
(74) Timme-Laragy, A. R.; Noyes, P. D.; Buhler, D. R.; Di Giulio, R. T. CYP1B1 knockdown does not alter synergistic developmental toxicity of polycyclic aromatic hydrocarbons in zebrafish (*Danio rerio*). *Mar. Environ. Res.* **2008**, *66*, 85−87.
(75) Fleming, C.; Di Giulio, R. The role of CYP1A inhibition in the embryotoxic interactions between hypoxia and polycyclic aromatic hydrocarbons (PAHs) and PAH mixtures in zebrafish (*Danio rerio*). *Ecotoxicology* **2011**, *20*, 1300−1314.